American Mineralogist, Volume 73, pages 1440–1448, 1988

Dorrite [$Ca_2(Mg_2Fe^{3+}_4)(Al_4Si_2)O_{20}$], a new member of the aenigmatite group from a pyrometamorphic melt-rock*

MICHAEL A. COSCA, ROLAND R. ROUSE, ERIC J. ESSENE
Department of Geological Sciences, University of Michigan, Ann Arbor, Michigan, 48109-1063, U.S.A.

ABSTRACT

Dorrite, a new mineral of the aenigmatite group, has been found in a paralava from the Powder River Basin, Wyoming. The type specimen used for X-ray analysis has been quantitatively analyzed, yielding the formula $(Ca_{1.92}Na_{0.07}K_{0.01})(Ca_{0.05}Mg_{1.05}Mn_{0.03}Fe^{2+}_{0.44}Ti_{0.05}Fe^{3+}_{4.38})(Fe^{3+}_{2.00}Al_{2.40}Si_{1.60})O_{20}$; the end-member formula is inferred to be $Ca_2(Mg_2Fe^{3+}_4)(Al_4Si_2)O_{20}$. The chemical compositions of individual dorrite grains within the same thin section display wide variations in tetrahedral Al/Fe^{3+}, but contain dominant Fe^{3+} in the octahedral sites and little Ti^{4+}. As is typical of aenigmatite-group minerals, dorrite is triclinic and twinned, producing a pseudomonoclinic symmetry. The space group is $P1$ or $P\bar{1}$ with refined parameters a = 10.505(3), b = 10.897(3), c = 9.019(1) Å, α = 106.26(2)°, β = 95.16(2)°, and γ = 124.75(2)°; V = 772.5(4) Å^3 (Z = 2) and ρ_{calc} = 3.959 g/cm^3. Dorrite has very strong absorption and high relief with approximate refractive indices of α = 1.82, β = 1.84, and γ = 1.86 (all ±0.01). Dorrite is nearly opaque in thin section, whereas in ultrathinned areas it displays the following pleochroic formula: X = red-orange to brown, Y = yellowish brown, and Z = greenish brown. It occurs as anhedral to prismatic grains up to 0.1 mm in length and in close association with esseneite or titanian andradite. Other minerals coexisting with dorrite include plagioclase, gehlenite-akermanite, and magnetite–magnesioferrite–spinel solid solutions, with lesser Ba-rich feldspar, wollastonite, ulvöspinel, nepheline, apatite, ferroan sahamalite, and secondary barite and calcite. The mineral is named for J. A. Dorr, Jr., late professor at the University of Michigan.

A series of mineral reactions relate dorrite + magnetite + clinopyroxene, rhönite + magnetite + olivine + clinopyroxene, and aenigmatite + pyroxene + olivine assemblages that are widespread in nature. The conditions necessary for crystallizing these assemblages appear restricted to low pressures and high temperatures. Dorrite is stable in strongly oxidizing, high-temperature, low-pressure environments.

INTRODUCTION

During a general investigation of pyrometamorphic melt-rock (paralava) in the Powder River Basin, Wyoming (Cosca et al., 1989), an aenigmatite-like mineral was identified based on chemical, optical, and X-ray powder-diffraction observations. Normalization of microprobe analyses results in the idealized formula $Ca_2Mg_2Fe^{3+}_4(Al_4Si_2)O_{20}$, although some grains revealed up to 75% replacement of tetrahedrally coordinated Al by Fe^{3+}. This phase is inferred to be isostructural with the aenigmatite group of minerals (aenigmatite, rhönite, serendibite, welshite, and krinovite plus synthetic "baikovite"), but is chemically most similar to rhönite [$Ca_2Mg_5Ti(Al_2Si_4)O_{20}$]. The lack of Ti and presence of dominant Fe^{3+} in octahedral coordination support its status as a new mineral. Phenocrysts or quenched crystals coexisting with this phase include plagioclase, gehlenite-akermanite, magnetite–magnesioferrite–spinel solid solutions, esseneite, nepheline, wollastonite, Ba-rich feldspar, apatite, ulvöspinel, ferroan sahamalite, and secondary barite, and calcite.

The mineral that we now call dorrite has apparently been described twice previously. The first report was from a basalt-limestone contact on Réunion Island (Havette et al., 1982). There it forms small, nearly opaque grains coexisting with melilite and titaniferous fassaite. It was labeled mineral X_1 and was found in association with mineral X_2 (probably a melanite garnet). The second report is from an investigation of a paralava from the Powder River Basin by Foit et al. (1987). They identified a mineral as Fe^{3+}-rich melilite, but the chemistry and optical properties of this "iron-melilite" are quite different from those of the melilite group and are similar to those of the rhönite-like phase described here. It appears that a rhönite-like phase was analyzed and mistakenly associated with a melilite X-ray pattern. In this paper we report data on the physical, chemical, and structural properties of a new rhönite-like mineral and discuss its relationship to previously described rhönites.

The sample described in this study (DR-8) comes from the Durham Ranch, located just east of Highway 59, about

* Contribution no. 454 from the Mineralogical Laboratory, Department of Geological Sciences, University of Michigan.

0003–004X/88/1112–1440$02.00

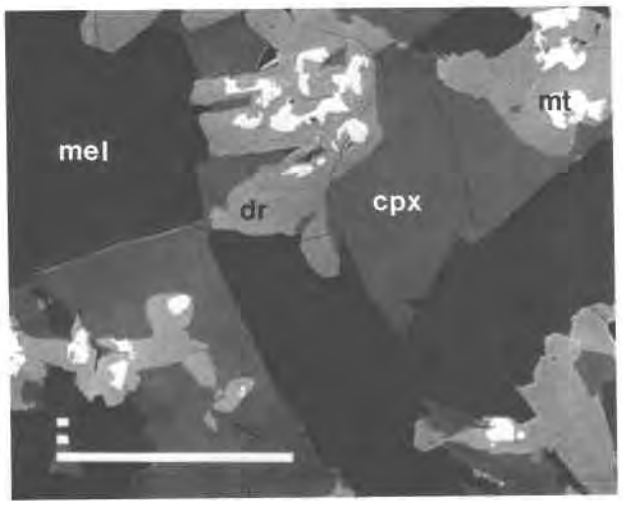

Fig. 1. Backscattered-electron photograph of dorrite (dr), clinopyroxene (cpx), magnetite (mt), and melilite (mel). Note textural disequilibrium of the magnetite inclusions. Scale bar = 100 μm.

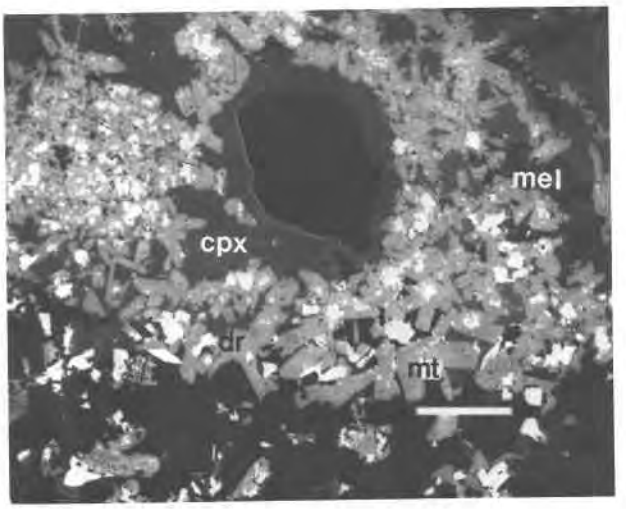

Fig. 2. Backscattered-electron photograph of dorrite forming around a vesicle. Symbols are the same as in Fig. 1. Scale bar = 100 μm.

13 km northeast of Reno Junction and 25 km south of Gillette, Wyoming. Rocks from this and other nearby localities form mesas that are separable into two distinct horizons. The lowest horizon is composed of unaltered sedimentary rocks, generally medium- to fine-grained siltstones, sandstones, and conglomerates. This horizon is overlain by a thick (1–30 m) capping of baked and reddened sedimentary rocks. Between the two horizons is a small zone of incompletely combusted coal and coal-ash–containing paralava. The paralava is a vesicular, slaglike rock that contains a variety of minerals with a variety of flow and quenched textures (Cosca et al., 1989).

The new mineral was named dorrite after Dr. John (Jack) A. Dorr, Jr., late professor of stratigraphy, paleontology, and regional geology at the University of Michigan. Dr. Dorr and his students conducted much of their research in Wyoming, and early in our study, he provided us with some locations of outcrops containing pyrometamorphic rock. The new mineral and mineral name were approved, prior to publication, by the IMA, Commission on New Minerals and Mineral Names. Type material is located in the Smithsonian Museum (NMNH 163357), and mineral grains used in the X-ray studies are housed in the mineral collections at the University of Michigan.

Petrography

In thin section, most dorrite grains display an intimate relationship with an esseneite-rich clinopyroxene ($CaFe^{3+}AlSiO_6$) that contains small amounts of diopside (Di), Ca Tschermak's component (CaTs), and/or Fe Tschermak's component (FTs) ($Di_{12-32}CaTs_{0-22}FTs_{0-19}$). Dorrite occurs most often within grains of clinopyroxene and in many cases forms pseudomorphs after clinopyroxene. In turn, many of the dorrite grains contain inclusions of primarily magnetite (Mt) that contains significant amounts of magnesioferrite (Mf) and spinel (Sp) ($Mt_{38-61}Mf_{17-43}Sp_{5-22}$). The magnetite inclusions are often quite irregular in outline, appearing to be partially consumed by reaction with the dorrite (Fig. 1). The dorrite grains containing the magnetic inclusions are often anhedral, whereas many of the grains without obvious magnetite inclusions are euhedral. Dorrite is also found in the presence of anorthite (An_{98}), but is generally found in close association with the assemblage clinopyroxene and magnetite. Clusters of dorrite grains sometimes develop around vesicles (Fig. 2).

A number of lobate, mainly crystalline domains of differing mineralogy are observable within the area of a thin section (Fig. 3). In cross section these domains display spherical and sinuous contacts, often outlined by oriented grains of melilite. The melilite is primarily gehlenite (Geh) but may contain significant amounts of akermanite (Ak) and sodium melilite (SM) ($Ak_{6-29}Geh_{60-87}SM_{2-18}$). The contacts between domains display evidence of reaction, possibly representing local boundaries between two or more different liquids (± crystals). The most extreme modal variations between these domains occur in the percentages of clinopyroxene and melilite, and dorrite is not found in regions of highest melilite concentration. However, where dorrite does occur with melilite, clinopyroxene is not found, and a phase with an empirical formula consistent with titanian andradite [$Ca_{3.00}(Fe^{2+}_{0.11}Mn_{0.02}Mg_{0.07}Fe^{3+}_{1.40}Ti^{4+}_{0.40})(Fe^{3+}_{0.08}Al_{0.36}Si_{2.56})O_{12}$] appears instead. Dorrites (and nearby clinopyroxenes) occuring in association with the garnet tend to be the most Fe rich. The mineral described as X_2, associated with rhönite and mineral X_1 (dorrite) by Havette et al. (1982) from a contact zone on Réunion Island, may also be a garnet. It also possible that mineral X_2 has a sphene-type structure. The low analytical totals of Havette et al. (1982) are also similar to our data and may indicate the presence of small amounts of OH substituting for O. With the

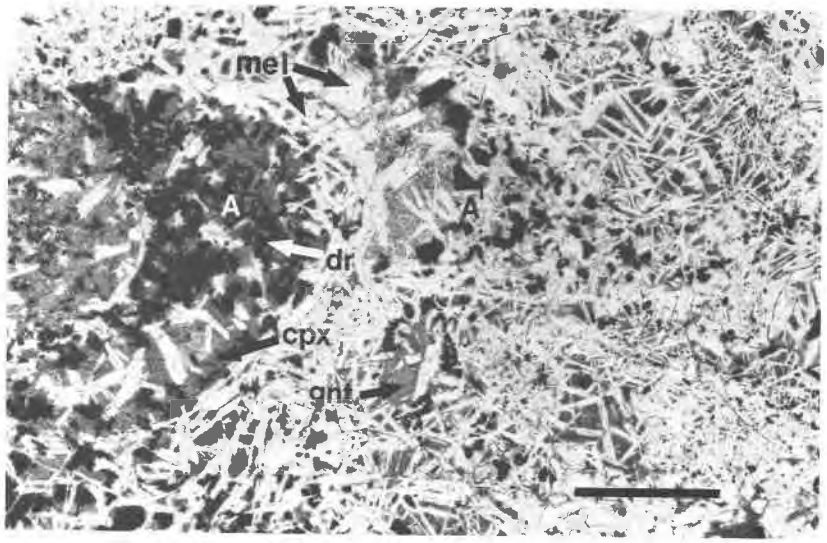

Fig. 3. Thin section, showing the distinct mineralogic zones referred to in the text. A–A′ shows the approximate location of the traverse across which the data in Tables 1 and 2 were collected. Scale bar = 2 mm.

exception of very small amounts of P, no additional elements were observed during a wavelength-dispersive scan of the Durham Ranch garnet.

Dorrite and associated phases in the type specimen (paralava DR-8) are preserved with quenched textures such as skeletal and hopper grains and often contain or form inclusions within other phases or in glass. Glass is found interstitially and often contains small crystals of apatite and smaller K-feldspar crystals visible only with backscattered-electron (BSE) imaging at high magnification. Along some grain boundaries, irregularly shaped pockets of quenched glass contain radiating crystals of Ba-rich feldspar ($Or_{9-16}Ab_{5-27}An_{42-73}Cn_{14-33}$), wollastonite ($Wo_{99}$), nepheline ($Ne_{83}Ks_{17}$), and magnetite (Mt)–jacobsite (Jb) solid solutions ($Mt_{82}Jb_{18}$) (Fig. 4). Barite and calcite appear in fractures and vesicle fillings but are interpreted to be secondary. In addition, small, highly reflective spheres of Fe-bearing sahamalite occur in some melilite.

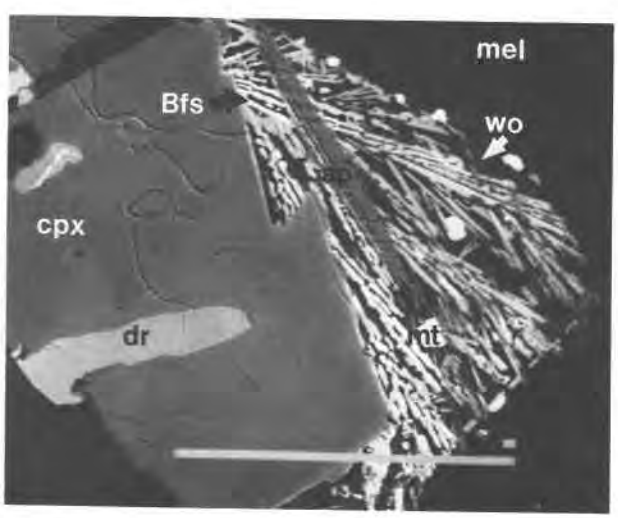

Fig. 4. Backscattered-electron photograph of barred Ba-rich feldspar (Bfs), wollastonite (wo), magnetite (mt), and apatite (ap) formed within an interstitial pocket of quenched liquid. Scale bar = 10 μm.

Chemistry

Chemical analyses of mineral grains were obtained from polished thin sections using a Cameca CAMEBAX microprobe, and these data are presented in Tables 1 and 2. Standard operating conditions consisted of an accelerating voltage of 15 kV and a sample current of 10 μA. A 1-μm-diameter electron beam was used for all analyses. The following well-characterized natural and synthetic phases were used as standards for quantitative analysis: hedenbergite for Ca, jadeite for Na, hornblende for K and Mg, rhodonite for Mn, ferrosilite for Fe, uvarovite for Cr, geikielite for Ti, and almandine for Al and Si. Counting times were set to a maximum of 30 s for most major elements and proved sufficient to obtain statistically significant results. All raw data were corrected for atomic number (*Z*), absorption (*A*), and fluorescence (*F*) using Cameca software. Because of the quenched textures, it was helpful to obtain images using backscattered-electron (BSE) imaging in order to isolate mineral grains for quantitative analysis. This technique was especially useful for distinguishing between intergrowths of pyroxene and dorrite.

In addition to chemical analyses obtained from polished thin sections, the single crystal used to obtain unit-cell parameters was also analyzed (Table 1). The crystal was carbon coated and a special sample holder was used that allowed placement of the crystal, still attached to a glass fiber, directly under the electron beam. The crystal was then rotated until a flat surface was obtained, and an analysis was performed. Because of the potential errors associated with this technique, such as a variable take-off

TABLE 1. Microprobe analyses of dorrite

	a	b	c	d	e	f	g	h	i
SiO_2	11.16	11.19	11.02	11.05	11.93	11.38	12.00	10.53	10.44
Al_2O_3	24.85	22.31	22.77	13.56	13.56	12.41	11.35	8.62	13.33
TiO_2	0.56	0.59	0.61	0.92	0.99	0.90	0.90	1.04	0.41
Cr_2O_3	0.05	0.26	0.07	0.00	0.00	0.04	0.02	0.01	0.01
Fe_2O_3	41.65	43.39	43.57	52.03	51.14	53.60	52.57	59.06	55.50
FeO	2.77	3.00	2.74	3.30	3.35	2.60	3.31	2.71	3.42
MnO	0.19	0.27	0.25	0.45	0.44	0.52	0.40	0.70	0.22
MgO	5.57	5.44	5.44	4.88	5.38	5.16	5.16	4.31	4.59
CaO	13.63	13.29	13.39	13.13	13.38	13.45	13.50	13.29	12.08
Na_2O	0.02	0.06	0.05	0.08	0.09	0.11	0.10	0.15	0.23
K_2O	0.02	0.02	0.02	0.02	0.03	0.02	0.01	0.01	0.03
Sum	100.47	99.82	99.93	99.42	100.29	100.19	99.32	100.43	100.26
Si	1.599	1.632	1.603	1.690	1.798	1.731	1.844	1.643	1.596
Al	4.196	3.835	3.903	2.445	2.408	2.225	2.055	1.584	2.403
Fe^{3+}	0.205	0.533	0.494	1.865	1.794	2.044	2.101	2.773	2.001
Fe^{3+}	4.286	4.229	4.275	4.125	4.007	4.093	3.978	4.159	4.386
Ti	0.060	0.065	0.067	0.105	0.112	0.103	0.104	0.122	0.046
Cr	0.006	0.029	0.008	0.000	0.000	0.005	0.003	0.001	0.000
Mg	1.189	1.183	1.180	1.112	1.209	1.169	1.181	1.002	1.048
Fe^{2+}	0.332	0.366	0.333	0.422	0.422	0.333	0.425	0.354	0.437
Mn	0.023	0.033	0.031	0.058	0.057	0.067	0.052	0.007	0.028
Ca	0.104	0.096	0.106	0.177	0.193	0.229	0.256	0.269	0.055
Ca	1.989	1.980	1.981	1.974	1.969	1.964	1.967	1.952	1.926
Na	0.007	0.016	0.015	0.023	0.026	0.033	0.031	0.045	0.068
K	0.004	0.004	0.004	0.003	0.005	0.003	0.002	0.003	0.006

Note: Analyses are from a traverse (A–A', Fig. 3) approximately 3 mm in length, across a sharp boundary separating modally distinct zones enriched in clinopyroxene (a–f) and melilite (g–h); see Fig. 5a. Also shown is the analysis of the single crystal used for the cell-parameter refinement (i). Formulae are calculated on the basis of 14 cations; FeO and Fe_2O_3 are recalculated from normalized formula.

angle, the results of the single-crystal analysis presented in Table 1 must be viewed with some caution. Our best estimate of the accuracy of this analysis is ±4% of the amount present for Fe, Mg, Al, and Si and perhaps twice that uncertainty for the other elements.

The analyses in Table 1 were used to define an ideal, end-member composition of dorrite as $Ca_2(Mg_2Fe^{3+}_4)(Al_4Si_2)O_{20}$. However, some Fe-rich grains (Table 1) are better represented by the ideal formula $Ca_2(Fe^{2+}_2Fe^{3+}_4)(Fe^{3+}_4Si_2)O_{20}$. The variation in chemical composition is due mainly to tetrahedral substitutions (Fig. 5a), where the inferred tetrahedral occupancies display a

TABLE 2. Clinopyroxene and garnet analyses

	Clinopyroxene						Garnet	
	a	b	c	d	e	f	g	h
SiO_2	29.82	29.79	30.74	29.79	27.24	26.88	30.21	30.67
Al_2O_3	16.81	17.60	14.01	12.54	11.58	9.58	4.46	3.30
TiO_2	1.22	0.98	1.54	1.97	2.35	2.39	6.02	5.14
Cr_2O_3	0.03	0.06	0.01	0.01	0.00	0.02	0.00	0.04
Fe_2O_3	24.85	24.24	24.69	27.81	31.88	34.65	23.68	25.95
FeO	0.86	0.77	1.74	1.55	0.97	0.76	0.00	0.00
MnO	0.19	0.15	0.14	0.23	0.19	0.31	0.19	0.20
MgO	2.65	2.76	2.90	2.90	2.02	1.92	0.51	0.56
CaO	23.31	23.30	23.20	23.00	22.73	22.59	32.99	32.94
Na_2O	0.23	0.18	0.29	0.21	0.17	0.17	0.02	0.01
K_2O	0.00	0.00	0.01	0.01	0.00	0.02	0.02	0.00
Sum	99.97	99.83	99.27	100.02	99.13	99.29	98.10	98.81
Si	1.198	1.195	1.251	1.218	1.143	1.139	2.568	2.602
Al	0.796	0.831	0.672	0.604	0.573	0.478	0.447	0.330
Ti	0.037	0.030	0.047	0.061	0.074	0.077	0.385	0.328
Cr	0.001	0.002	0.000	0.000	0.000	0.001	0.000	0.000
Fe^{3+}	0.751	0.732	0.755	0.856	1.007	1.105	1.513	1.660
Mg	0.159	0.165	0.176	0.177	0.126	0.121	0.065	0.071
Fe^{2+}	0.029	0.026	0.059	0.053	0.034	0.027	0.000	0.000
Mn	0.007	0.005	0.005	0.008	0.007	0.011	0.013	0.013
Ca	1.004	1.001	1.011	1.007	1.022	1.026	3.005	2.994
Na	0.018	0.013	0.023	0.016	0.014	0.014	0.002	0.002
K	0.000	0.000	0.001	0.000	0.000	0.001	0.002	0.000

Note: Letter labels of columns denote grains that coexist with corresponding dorrites from Table 1. Formulae are calculated on the basis of cations (pyroxene = 4; garnet = 8). FeO and Fe_2O_3 are recalculated from normalized formula.

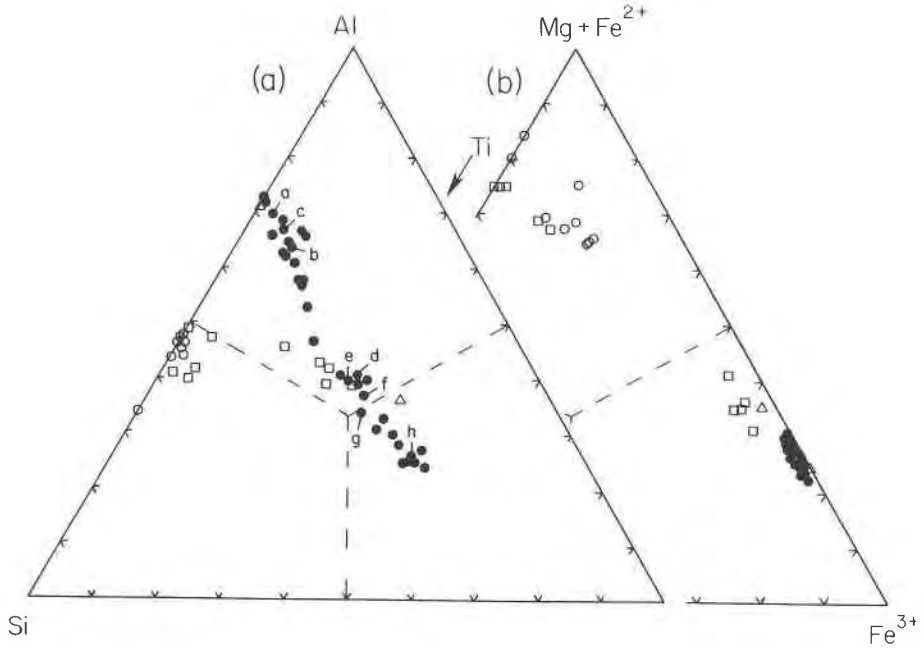

Fig. 5. (a) Tetrahedral occupancy of dorrites compared to rhönites in the literature. Dorrites are from this study (filled circles), Havette et al. (1982) (squares), and Foit et al. (1987) (triangles). Rhönite analyses (open circles) contain <1.0 wt% Na_2O and were taken from the following: Soellner, 1907; Babkine, 1964; Cameron et al., 1970; Fuchs, 1971; Grünhagen and Seck, 1972; Kyle and Price, 1975; Magothier and Velde, 1976; Olsson, 1983; and Nishio et al., 1985. (b) Octahedral occupancy of dorrites compared to rhönites in the literature [sources of data and symbols are the same as in (a)].

range in $Fe^{3+}/(Fe^{3+} + Al)$ from 0.2 to 0.7. This chemical variation occurs over a distance of approximately 3.0 mm and is transitional across a sharp boundary separating zones enriched primarily in either melilite or clinopyroxene (Fig. 3). The exchange $Fe^{3+} = Al$ occurs with a nearly constant ratio of $Si/(Si + Al + Fe^{3+}) = 0.27$. Figure 5a reflects the maximum chemical range exhibited by the dorrite examined in this study.

The calculated octahedral occupancies of dorrite display very little variation, ranging between 68 and 75% Fe^{3+} (Fig. 5b). Similar results are obtained from the data of Havette et al. (1982) and Foit et al. (1987). These values greatly exceed those of rhönites, which exhibit a range from 0 to 20%; a 30% octahedral-site occupancy of Fe^{3+} is calculated from a rhönite presented by Johnston and Stout (1985), although their analysis indicates solid solution toward aenigmatite.

Comparison of rhönite and dorrite compositions taken from the literature to those obtained in this study (Fig. 5) reveal patterns possibly indicating a solvus between these two minerals. This could explain the restricted compositional variations thus far shown for these chemically and structurally similar phases. A dorrite-rhönite solvus may also be indicated by the observations of Havette et al. (1982) of a close association between rhönite and their mineral X_1.

Because the structures of dorrite and rhönite have not yet been determined, the degree of cation ordering (if any) in these phases remains unknown. However, the structure of aenigmatite is known (Cannillo et al., 1971), and assuming this mineral is isostructural with dorrite (as indicated by our data), similar crystal-chemical results may apply. Cannillo et al. (1971) refined the tetrahedral occupancies of aenigmatite; their results indicate a strong preference of Si for two of the six tetrahedral sites. Small amounts of Fe^{3+} are subequally distributed in the remaining four tetrahedral sites. Based on the regular variation of tetrahedral occupancy inferred from our microprobe data, similar ordering of Si may be expected in the tetrahedral sites of dorrite. Cannillo et al. (1971) also provided evidence that Ti is largely ordered in the smallest of the seven octahedral sites, with lesser ordering of Ti and Fe^{2+} in the remaining ones. Although generally restricted to eightfold coordination, small amounts of Ca were inferred to occupy the octahedral sites in aenigmatite (Cannillo et al., 1971). This is consistent with similar assignments inferred from microprobe analyses of dorrite (Table 1). The small amount of sixfold-coordinated Ca may reflect distortions (expansion) of the octahedral site associated with the high-temperature environments in which these minerals form.

Dorrite is chemically related to rhönite by the following coupled substitutions:

$$^{[6]}R^{2+}{}^{[4]}Si = {}^{[6]}R^{3+}{}^{[4]}R^{3+} \quad (1)$$

and

$$^{[6]}R^{2+}{}^{[6]}Ti = {}^{[6]}R^{3+}{}^{[6]}R^{3+} \quad (2)$$

where R^{2+} is Fe^{2+} or Mg and R^{3+} is Al or Fe^{3+}. These exchanges are shown schematically in Figure 6, projected in terms of theoretical end members. The two previously described dorrites are shown in Figure 6 and include mineral X_1 from Réunion Island (Havette et al., 1982) and the "iron melilite" of Foit et al. (1987). If solid solution toward aenigmatite is small (<1.0 wt% Na_2O), this projection is useful to distinguish rhönite from dorrite and indicates the types of solid solutions that may be anticipated. Rhönites containing significant Na (e.g., Kyle and Price, 1975; Johnston and Stout, 1985) are excluded from this diagram. Compositions with greater than one Ti cation per formula unit are not properly represented on this diagram because they require an additional exchange such as $NaTi = CaR^{3+}$, or $CaTi = MgSi$ for the most Ti-rich rhönite from the Allende meteorite (Fuchs, 1971); a lower-valence state for Ti (Fuchs, 1978; Beckett et al., 1986) and hence a different substitutional scheme are also possible for the Allende rhönite.

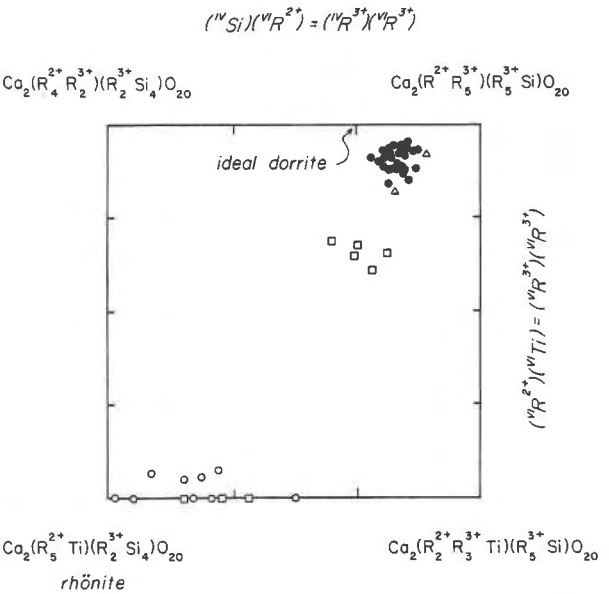

Fig. 6. Compositional variation of dorrites and rhönites obtained from this study and taken from the literature plotted in terms of hypothetical end members (sources of data and symbols are the same as in Fig. 5a).

Physical and optical properties

Dorrite forms small prismatic crystals up to 0.1 mm long. Crystals are dark red-brown to dark brown in color, have a submetallic luster, and are nearly opaque except in very thin crystals (<15 μm). Some grains exhibit good cleavages that are assumed parallel to {010} and {001} by analogy to the other members of the aenigmatite group. The Mohs hardness, determined by crushing hand-picked grains between polished slabs of apatite, is approximately 5. The scratches were confirmed in the apatite with the aid of a binocular microscope. Grains are brittle when crushed, have an irregular fracture, and leave a gray streak. The volume directly obtained from the crystal used in the unit-cell refinement is 772.5(4) Å^3. Based on the chemical composition of this grain (Table 1), the density was calculated as 3.959 g/cm^3. Density was not measured because most of the grains contain inclusions of magnetite that preclude an accurate measurement. The volume of the end-member dorrite is 769 Å^3. This was estimated by extrapolating the volume of the dorrite solid solution with small amounts of isostructural pyroxenes to obtain an end-member formula $Ca_2(Mg_2Fe_4^{3+})(Al_4Si_2)O_{20}$. Similarly, a volume for the Fe-rich composition of dorrite $[Ca_2(Fe_2^{2+}Fe_4^{3+})(Fe_4^{3+}Si_2)O_{20}]$ has been calculated as 816 Å^3. The calculation assumes that variations in the molar volume of dorrite are well represented by changes in equivalent amounts of pyroxenes, that volumes of clinopyroxene vary linearly, and that no significant excess molar volumes occur.

The optical properties of dorrite have been determined in oils by using separated mineral grains. These properties are difficult to measure because of the extreme absorption exhibited by this mineral even under an intense (white) light source. Consequently the optic figures were usually diffuse, although they were sometimes adequate to determine the optical orientation. The refractive indices were measured as the following: $\alpha = 1.82$, $\beta = 1.84$, and $\gamma = 1.86$ (all ± 0.01). The dorrite from an ultrathin thin section displayed a large, negative $2V$ of approximately 90°, consistent with the very approximate refractive indices. Pleochroism is only observed in ultrathinned thin sections or small grains and is very strong with the formula X = red-orange brown, Y = yellowish brown, and Z = greenish brown. Though probably present, dispersion could not be observed owing to the strong absorption.

Crystallography

The unit cell and space group of dorrite were obtained using the precession and cone-axis methods and a Syntex $P2_1$ single-crystal diffractometer. A set of four precession levels showed what appeared to be a monoclinic intensity distribution and a C-centered cell of dimensions $a = 9.98$, $b = 5.08$, $c = 5.24$ Å, and $\beta = 99.9°$. However, a cone-axis photograph with a as the precessing axis revealed additional very weak levels requiring a doubling of a. A photograph of the first superstructure level parallel to the b^*c^* plane showed that there were two additional lattice points per cell, requiring that the b and c parameters also be doubled. Comparison of the dorrite reciprocal lattice with the reciprocal lattice diagrams of twinned and untwinned krinovite (Merlino, 1972) proved conclusively that dorrite is triclinic-pseudomonoclinic and twinned by a twofold rotation about the pseudomonoclinic b axis. Such twinning is the rule in minerals of the aenigmatite group. Merlino (1972) also tabulated the parameters of the three alternative pseudomonoclinic unit cells that have been used by various workers for aenigmatite, krinovite, and rhönite and also the parameters of the true, untwinned triclinic cell of the Delauney type. The pseudo-

TABLE 3. X-ray powder diffraction data for dorrite

I_{obs}	d_{obs}	d_{calc}	hkl	I_{obs}	d_{obs}	d_{calc}	hkl
20	8.1	8.21	001	5	2.257	2.271	$\bar{2}41$
		8.19	100			2.269	223
		8.19	010			2.264	$24\bar{3}$
20	7.5	7.51	$0\bar{1}1$			2.256	$14\bar{3}$
5	6.4	6.53	$1\bar{1}1$			2.245	$\bar{2}23$
10	4.87	4.89	$11\bar{1}$	5	2.205	2.209	310
		4.89	011			2.209	130
5	4.39	4.28	$2\bar{2}1$			2.207	$04\bar{1}$
5	4.22	4.25	$10\bar{2}$			2.206	$\bar{4}41$
		4.24	$20\bar{1}$			2.202	$\bar{1}32$
10	3.46	3.47	$\bar{2}12$			2.202	$\bar{4}32$
100	2.971	2.992	120	60	2.125	2.140	$44\bar{2}$
		2.992	210			2.134	$4\bar{1}1$
		2.985	013			2.130	$25\bar{1}$
		2.975	$0\bar{3}1$			2.125	$\bar{2}04$
		2.954	$\bar{2}31$			2.099	$03\bar{4}$
5	2.895	2.918	$11\bar{3}$			2.096	$04\bar{3}$
		2.886	$10\bar{3}$			2.091	$\bar{3}50$
		2.882	$\bar{3}12$			2.093	$32\bar{3}$
5	2.815	2.816	$\bar{1}22$			2.092	$\bar{5}30$
	2.705	2.719	$24\bar{1}$	20	2.035	2.041	$\bar{5}40$
		2.706	$20\bar{3}$			2.041	$45\bar{0}$
		2.704	$1\bar{1}3$			2.031	$\bar{4}23$
		2.701	$30\bar{2}$	5	1.842		
80	2.558	2.560	$21\bar{3}$	20	1.737		
		2.560	$\bar{1}13$	10	1.695		
80	2.515	2.527	202	15	1.626		
		2.521	211	20	1.613		
5	2.453	2.458	$22\bar{1}$	20	1.544		
		2.452	$43\bar{1}$	30	1.511		
		2.446	$22\bar{2}$	30	1.482		
		2.446	022	5	1.456		
10	2.349	2.361	$14\bar{0}$	5	1.432		
		2.361	$31\bar{1}$				
		2.356	$4\bar{4}0$				
		2.345	$\bar{4}22$				
		2.338	$30\bar{3}$				
		2.334	$31\bar{2}$				

Note: Data were obtained with a 114.6-mm-Gandolfi camera, Mn-filtered Fe$K\alpha$ radiation, and a Si internal standard. Intensities were visually estimated.

monoclinic cell of dorrite having $a = 19.97$, $b = 30.17$, $c = 10.48$ Å, and $\beta = 99.9°$ found in this study is the "OF (Olsen-Fuchs) cell" in Merlino's terminology.

Using the above information and the diffractometer data of the same crystal, the true (untwinned) cell of dorrite was found to be triclinic, $P1$ or $P\bar{1}$, with refined parameters $a = 10.505(3)$, $b = 10.897(3)$, $c = 9.019(1)$ Å, $\alpha = 106.26(2)°$, $\beta = 95.16(2)°$, and $\gamma = 124.75(2)°$. The unit-cell volume for this crystal ($Z = 2$) is 772.5(4) Å^3; the axial ratio a:b:c is 0.9640:1:0.8277. The transformation matrices between the triclinic cell and the various pseudomonoclinic cells are given by Merlino (1972).

X-ray powder-diffraction data from approximately 12 hand-picked grains of dorrite were obtained using a 114.6-mm-diameter Gandolfi camera, Mn-filtered Fe$K\alpha$ radiation, and elemental Si as an internal standard. The sample used for the Gandolfi photograph was polycrystalline, as individual crystals were too small to give a usable photograph. Indexed reflections and intensities from this pattern are presented in Table 3. Reflections were indexed by least-squares refinement of the observed d values together with the independently determined unit-cell data. An attempt was made to refine the triclinic cell parameters of dorrite from the powder data alone, but the results were unsatisfactory owing to the small number of reflections that could be unambiguously indexed.

DISCUSSION

Occurrences of rhönite and aenigmatite are generally restricted to silica-undersaturated, mafic to intermediate, extrusive and intrusive alkalic rocks (Deer et al., 1978). From these reports emerges a pattern of a near-ubiquitous association of either rhönite or aenigmatite in natural parageneses coexisting with olivine, magnetite (or spinel solid solutions), and clinopyroxene. Nearly all published descriptions of rhönite contain coexisting olivine (usually intermediate to fayalitic), clinopyroxene (usually titanian augite or fassaite), and a spinel solid solution (often Ti-rich magnetite) (e.g., LaCroix, 1909; Yagi, 1953; Ficke, 1961; Babkine et al., 1964; Cameron et al., 1970; Fuchs, 1971; Brooks et al., 1979; Havette et al., 1982; Olsson, 1983; Johnston and Stout, 1985). Similar associations are described occurring with aenigmatite, but in these descriptions the clinopyroxene is usually aegirine or a titanian, sodic augite (e.g., Carmichael, 1962; Abbott, 1967; Lindsley et al., 1971; Platt and Woolley, 1986; Stolz, 1986; Jorgensen, 1987). A similar association now exists for the mineral dorrite (Havette et al., 1982; Foit et al., 1987; Cosca et al., 1989). The repeated observation of associated phases suggests similarities in the conditions required for generating aenigmatite-, rhönite-, and dorrite-bearing assemblages.

Abbott (1967) suggested that the following qualitative conditions are necessary for the formation of aenigmatite: (1) relatively high concentrations of TiO_2, (2) peralkalinity, and (3) low oxygen fugacity. Lindsley (1971) placed quantitative limits on the stability of aenigmatite and restricted its occurrence to a temperature of >750 °C, a pressure of <0.5 kbar, and oxygen fugacities below the Ni-NiO oxygen buffer. Although aenigmatite may be synthesized at the above temperature and pressure at the Ni-NiO oxygen buffer (Lindsley, 1971), with time (five months in his experiments) when subjected to the above conditions, the aenigmatite breaks down completely to acmite + Ti-rich magnetite + quartz. These reaction products are probably the result of an oxidation-reduction equilibrium such as the following reaction proposed by Marsh (1975):

$$3Na_2Fe^{2+}_5TiSi_6O_{20} + 2O_2 = 6NaFe^{3+}Si_2O_6 + 6SiO_2 + 3Fe_2TiO_4 + Fe^{2+}Fe^{3+}_2O_4. \quad (3)$$

Thus, aenigmatite appears sensitive to changes in fO_2 and is restricted to oxygen fugacities below that of the Ni-NiO buffer (Lindsley, 1971).

Although the occurrence of aenigmatite in natural parageneses is generally assumed to be the result of an

oxidation reaction involving aegirine and a sodic liquid (e.g., Nicholls and Carmichael, 1969), a series of simple solid-solid reactions may also be written relating the stability of aenigmatite, dorrite, and rhönite relative to pyroxenes, olivines, spinels, and/or oxides and appears to especially well represent rhönite and dorrite occurrences in nature. For example, aenigmatite may form from a pyroxene component and olivine by the reaction

$$2NaFe^{2+}_{0.5}Ti_{0.5}Si_2O_6 + 2Fe_2SiO_4 = Na_2Fe^{2+}_5TiSi_6O_{20}. \quad (4)$$

Rhönite and dorrite may be viewed as Ca analogues to the aenigmatite in Reaction 4. The stability of end-member rhönite $Ca_2Mg_5Ti(Al_2Si_4)O_{20}$ is limited by the following reactions:

$$[CaAlSiAlO_6 + CaMgSi_2O_6] + Mg_2TiO_4 + Mg_2SiO_4 = Ca_2Mg_5Ti(Al_2Si_4)O_{20} \quad (5)$$

and

$$[CaAlTiAlO_6 + CaMgSi_2O_6] + 2Mg_2SiO_4 = Ca_2Mg_5Ti(Al_2Si_4)O_{20}. \quad (6)$$

If thermodynamic data were available for rhönite and adequate mixing parameters were available for pyroxene, olivine, and rhönite, such reactions could be used to define the stability limits of rhönite in parageneses involving these minerals. Unfortunately, no thermodynamic data and only very limited experimental data (Boivin, 1980; Kunzmann et al., 1986) exist for rhönite that could be used to constrain its stability. Preliminary experimental data of Kunzmann et al. (1986) for an olivine nephelinite bulk composition suggest that rhönite forms at supersolidus conditions at very low pressure. These conditions are consistent with most reports of rhönite, which usually describe it as a late-stage crystallization product of alkaline lavas (e.g., Soellner, 1907; LaCroix, 1909; Ficke, 1961; Brooks et al., 1979; Kyle and Price, 1975; Olsson, 1983; Johnston and Stout, 1985) and intrusive rocks (Tomita, 1934; Cameron et al., 1970). In occurrences where textural evidence supports rhönite as a near-liquidus phase, it is rimmed by an unidentified opaque mineral (Cameron et al., 1970) or by aenigmatite (Yagi, 1953), possibly indicating that rhönite may have a somewhat higher thermal stability than aenigmatite.

In all rhönite analyses except those from the Allende meteorite (Fuchs, 1971; 1978) significant Fe^{3+} is present, suggesting that rhönite is stable under relatively oxidizing conditions. Dorrite, on the other hand, contains even greater proportions of Fe^{3+} and possibly indicates stability limits of higher oxygen fugacity. This inference is consistent with previous estimates of oxygen fugacity for Wyoming paralava to be near the hematite-magnetite buffer (Cosca and Peacor, 1987). The two geologic environments from which dorrite has been described attest to the relatively rare conditions necessary for its crystallization. End-member dorrite may be limited by a reaction such as the following:

$$2CaFe^{3+}_2SiO_6 + 2MgAl_2O_4 = Ca_2(Mg_2Fe^{3+}_4)(Al_4Si_2)O_{20} \quad (7)$$

The ΔV for Reaction 7 has been calculated as 14 cm^3, confirming that dorrite is the phase favored by low pressure. This result is in agreement with the physical environment containing dorrite and also with textures observed in paralavas, where dorrites appear to be replacing magnetite-spinel solid solutions. The most Fe^{3+}-rich dorrites in paralava may be produced when accompanied by increased magnetite solid solution as represented by the reaction

$$2CaFe^{3+}_2SiO_6 + 2Fe^{2+}Fe^{3+}_2O_4 = Ca_2(Fe^{2+}_2Fe^{3+}_4)(Fe^{3+}_4Si_2)O_{20}. \quad (8)$$

The ΔV for this reaction is estimated to be 19 cm^3, again indicating that the aenigmatite-group phase is stable at low pressures.

Where rhönite has been reported with aenigmatite (Yagi, 1953), rhönite forms cores surrounded by discontinuously zoned aenigmatite and perhaps reflects variations in temperture and oxidation state with time. A similar phenomenon may be represented by the coexistence of rhönite and dorrite (Havette et al., 1982) in separate zones of the basalt-limestone contact on Réunion Island. Dorrite, rhönite, and aenigmatite all form at very low pressures and at high temperatures in rocks of alkaline bulk composition. In paralava, dorrite appears to be favored over rhönite formation because of the high oxidation state and by the general absence of Ti in the sedimentary rocks melting to form paralava.

Note added in proof. The crystal structure of an Fe^{3+}-rich synthetic dorrite and its relation to aenigmatite-group minerals have recently been described by Mumme (1988, Neues Jahrbuch für Mineralogie Monatshefte, 359–366). These crystal-structure results compare favorably with our data and indicate that small variations in the unit-cell parameters of dorrite occur with increased Fe^{3+} substitution. The composition reported by Mumme (1988) plots close to the upper right-hand corner of Figure 6.

Acknowledgments

We thank W. M. Butler of the Chemistry Department, University of Michigan, for collecting data with the four-circle X-ray diffractometer. D. R. Peacor is thanked for helpful discussions, and for reviewing an earlier manuscript. C. H. Henderson is acknowledged for maintaining the electron microscope in excellent working order. A review by F. F. Foit, Jr., and comments by J. A. Mandarino on behalf of the IMA are both gratefully acknowledged. The electron microprobe used in this study was acquired under NSF grant EAR-82-12764. Parts of this research have been supported by NSF grant EAR-84-08168 to E.J.E.

References cited

Abbott, M.J. (1967) Aenigmatite from the groundmass of a peralkaline trachyte. American Mineralogist, 52, 1896–1901.

Babkine, J., Conquére, F., Vilminot, J.C., and Duong, P.K. (1964) Sur un nouveau gisement de rhönite (Monistrol-d'Allier, Haute Loire). Comptes Rendus Hebdomadaires des Seances de l'Academie des Sciences, 258, 5479–5481.

Beckett, J.R., Grossman, L., and Haggerty, S.E. (1986) Origin of Ti^{3+}-bearing rhönite in Ca-, Al-rich inclusions: An experimental study. Meteoritics, 21, 332–333.

Boivin, P. (1980) Données expérimentales preliminaires sur la stabilité

de la rhönite à 1 atmosphere: Application aux gisements naturels. Bulletin de Minéralogie, 103, 491–502.

Brooks, C.K., Pedersen, A.K., and Rex, D.C. (1979) The petrology and age of alkaline mafic lavas from the nunatak zone of central East Greenland. Grønlands Geologiske Undersøgelse Bulletin, 133, 1–28.

Cameron, K.L., Carman, M.F., and Butler, J.C. (1970) Rhönite from Big Bend National Park, Texas. American Mineralogist, 55, 864–874.

Cannillo, E., Mazzi, P.D., Fang, J.H., Robinson, P.D., and Ohya, Y. (1971) The crystal structure of aenigmatite. American Mineralogist, 56, 427–446.

Carmichael, I.S.E. (1962) Pantelleritic liquids and their phenocrysts. Mineralogical Magazine, 33, 86–113.

Cosca, M.A., and Peacor, D.R. (1987) Chemistry and structure of esseneite ($CaFe^{3+}AlSiO_6$), a new pyroxene produced by pyrometamorphism. American Mineralogist, 72, 148–156.

Cosca, M.A., Essene, E.J., Geissman, J.G., Simmons, W.B., and Coates, D.A. (1989) Pyrometamorphic rocks associated with naturally burned coal beds, Powder River Basin, Wyoming. American Mineralogist, 74, in press.

Deer, W.A., Howie, R.A., and Zussman, J. (1978) Rock-forming minerals (2nd edition), vol. 2A, p. 640–658. Wiley, New York.

Ficke, B. (1961) Petrologische Untersuchungen an Tertiaren bsaltischen bis phonolithischen Vulkaniten der Rhön. Tschermaks Mineralogische und Petrographische Mitteilungen, 7, 337–436.

Foit, F.F., Hooper, R.L., and Rosenberg, P.E. (1987) An unusual pyroxene, melilite, and iron oxide mineral assemblage in a coal-fire buchite from Buffalo, Wyoming. American Mineralogist, 72, 137–147.

Fuchs, L.H. (1971) Occurrence of wollastonite, rhönite, and andradite in the Allende meterorite. American Mineralogist, 56, 2053–2068.

——— (1978) The mineralogy of a rhönite-bearing calcium-aluminum–rich inclusion in the Allende meteorite. Meteoritics, 13, 73–87.

Grünhagen, H., and Seck, H.A. (1972) Rhönit aus einem Melaphonolith vom Puy de Saint-Sandoux (Auvergne). Tschermaks Mineralogische und Petrographische Mitteilungen, 18, 17–38.

Havette, A., Clocchiatti, R., Nativel, P., and Montaggioni, L. (1982) Une paragenèse inhabituelle à fassaïte, mélilite et rhönite dans un basalte alcalin contaminé au contact d'un récif corallien (Saint-Leu, Ile de la Réunion). Bulletin de Minéralogie, 105, 364–375.

Johnston, A.D., and Stout, J.H. (1985) Compositional variation of naturally occurring rhoenite. American Mineralogist, 70, 1211–1216.

Jorgenson, K.A. (1987) Mineralogy and petrology of alkaline granophyric xenoliths from the Thorsmork ignimbrite, southern Iceland. Lithos, 20, 153–168.

Kunzmann, T., Spicker, G., and Huckenholz, H.G. (1986) Stabilität von Rhönit in natürlichen und synthetischen Paragenesen (abs.). Fortschritte der Mineralogie, 64, 92.

Kyle, P.R., and Price, R.C. (1975) Occurrences of rhönite in alkalic lavas of the McMurdo Volcanic Group, Antarctica, and Dunedin Volcano, New Zealand. American Mineralogist, 60, 722–725.

LaCroix, M.A. (1909) Note sur la rhönite du Puy de Barneire à Saint-Sandoux. Bulletin de Société Française de Minéralogie et de Cristallographie, 32, 325–331.

Lindsley, D.H. (1971) Synthesis and preliminary results on the stability of aenigmatite ($Na_2Fe_5TiSi_6O_{20}$). Carnegie Institution of Washington Year Book 70, 188–190.

Lindsley, D.H., Smith, D., and Haggerty, S.E. (1971) Petrology and mineral chemistry of a differentiated flow of Picture Gorge basalt near Spray, Oregon. Carnegie Institution of Washington Year Book 70, 264–285.

Magonthier, M.C., and Velde, D. (1976) Mineralogy and petrology of some Tertiary leucite-rhönite basanites from central France. Mineralogical Magazine, 40, 817–826.

Marsh, J.S. (1975) Aenigmatite stability in silica-undersaturated rocks. Contributions to Mineralogy and Petrology, 50, 135–144.

Merlino, S. (1972) X-ray crystallography of krinovite. Zeitschrift für Kristallographie, 136, 81–88.

Nicholls, J., and Carmichael, I.S.E. (1969) Peralkaline acid liquids: A petrological study. Contributions to Mineralogy and Petrology, 20, 268–294.

Nishio, F., Katsushima, T., and Ohmae, H. (1985) Volcanic ash layers in bare ice areas near the the Yamato Mountains, Dronning Maud Land and the Allan Hills, Victoria Land, Antarctica. Annals of Glaciology, 7, 34–41.

Olsson, H.B. (1983) Rhönite from Skåne (Scania), southern Sweden. Geologiska Föreningens i Stockholm Förhandlingar, 105, 281–286.

Platt, R.G., and Woolley, A.R. (1986) The mafic mineralogy of the peralkaline syenites and granites of the Mulanje complex, Malawi. Mineralogical Magazine, 50, 85–99.

Soellner, J. (1907) Über Rhönite, ein neues änigmatitähnliches Mineral und über die verbreitung desselbenin basaltischen Gesteinen. Neues Jahrbuch für Mineralogie Abhandlungen, 24, 475–547.

Stolz, A.J. (1986) Mineralogy of the Nandewar volcano, northeastern New South Wales, Australia. Mineralogical Magazine, 50, 241–255.

Tomita, T. (1934) On kaersutite from Dogo, Oki Islands, Japan, and its magmatic alteration and resorption. Journal of the Shanghai Scientific Institute, 1, 99–136.

Yagi, K. (1953) Petrochemical studies of the alkalic rocks of the Morotu district, Sakhalin. Geological Society of America Bulletin, 64, 769–809.

Manuscript received January 14, 1988
Manuscript accepted July 29, 1988